

# Design techniques for switched capacitor adaptive line equalizer

著者	Nakayama Kenji, Sato Yayoi, Kuraishi Yoshiaki
journal or publication title	IEEE transactions on circuits and systems
volume	CAS-32
number	8
page range	759-766
year	1985-08-01
URL	<a href="http://hdl.handle.net/2297/3948">http://hdl.handle.net/2297/3948</a>

# Design Techniques for Switched-Capacitor Adaptive Line Equalizer

KENJI NAKAYAMA, SENIOR MEMBER, IEEE, YAYOI SATO, AND YOSHIAKI KURAISHI

**Abstract**—This paper describes design techniques for a switched capacitor adaptive line equalizer which is applied to high speed (200 kb/s) digital transmission over analog subscriber loops. An equalizer transfer function is approximated so as to minimize intersymbol interference of an isolated pulse response. Optimum pole-zero location, which is suited to line characteristics in a wide frequency band, is also discussed. In order to attain high accuracy capacitor ratios using a small unit capacitor, capacitor values are rounded off into equivalent integer values, and are discretely optimized using pole-zero deviation as an error criterion. The equalizer has a finite number of frequency responses which correspond to line lengths. Gain and delay time differences between the adjoining step responses are compressed. The designed switched capacitor line equalizer was fabricated using 3- $\mu$ m CMOS technology. Measured data were very close to designed performances.

## I. INTRODUCTION

**A**DVANCEMENT in digital transmission networks and increase in information to be supplied have promoted the development of digital transmission systems utilizing analog subscriber loops [1], [2]. Furthermore, recent LSI technology will make it possible to develop economical and compact digital subscriber transmission systems [3]. Among many technical objectives to be overcome, development of an LSI line equalizer system seems to be most important.

Switched-capacitor (SC) circuits are very suited to realizing the line equalizer on a monolithic MOS circuit with a small chip area and a low power consumption [4]–[7]. One hopeful approach to varying SC circuit characteristics is to discretely change capacitor values using a programmable capacitor array [8]. This kind of variable SC circuit, therefore, has a finite number of step responses. These step responses are individually optimized for the corresponding transmission-line lengths. In order to successfully apply the SC adaptive equalizer to long length transmission lines and high-speed digital transmission, the following technical objectives must be solved. They include transfer function optimization with intersymbol interference as an error criterion, reduction in a total amount of capacitors and compressing gain and delay time differences between the adjoining step responses.

This paper provides design techniques for the SC adaptive line equalizer, which is applied to the time compression multiplexed bidirectional digital transmission over

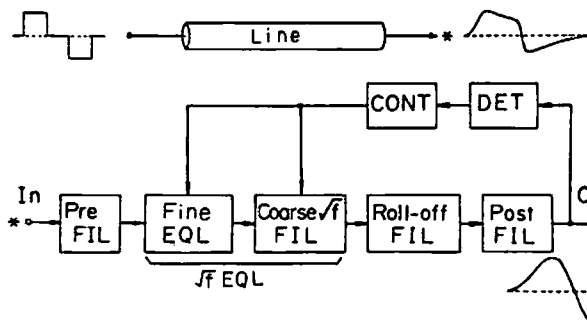


Fig. 1. Adaptive line equalizer system.

analog subscriber loops [9]. Bit rate is 200 kb/s and line loss at the Nyquist frequency is up to 45 dB. Discussions in this paper are mainly directed toward the mentioned objectives.

Section II briefly describes a functional block diagram for a line equalizer system. In Section III, an approximation algorithm for an equalizer transfer function is provided. Reductions in the gain and delay time differences are discussed in Section IV. Section V describes configurations for SC equalizers. A discrete optimization algorithm for capacitor values is provided in Section VI. Finally, Section VII presents examples for designed equalizer characteristics and fabricated LSI performance.

## II. SYSTEM DESCRIPTION

Fig. 1 shows a functional block diagram for an adaptive line equalizer system. Bipolar coded digital signals having 50-percent duty rectangular pulses are transmitted through the analog subscriber loops. The transmitted pulse is greatly distorted by the line characteristics. In other words, intersymbol interference (ISI) results, and error rate  $q$  in terms of a signal-to-noise ratio is highly degraded. Before detecting the received pulse, it is optimally shaped through the line equalizer system. Generally speaking, line characteristics are equalized by a  $\sqrt{f}$  equalizer, and its output waveform is shaped so as to minimize ISI through a roll-off filter.

The  $\sqrt{f}$  EQL and the roll-off filter are realized with SC circuits. Therefore, a pre-filter and a post-filter are used for anti-aliasing and smoothing waveforms, respectively. The  $\sqrt{f}$  EQL consists of a coarse  $\sqrt{f}$  EQL and a fine  $\sqrt{f}$  EQL. The line characteristics are mainly equalized by the coarse  $\sqrt{f}$  EQL. The fine EQL, which has approximate flat

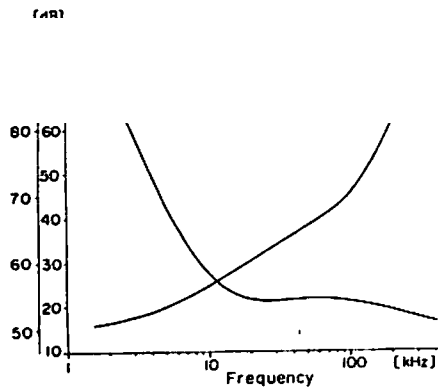


Fig. 2. Frequency responses for 0.5-mm  $\varnothing$  line with 5.9-km length (45-dB loss at 100 kHz).

plitude responses, is used for further adjusting gain differences between the adjoining step responses of the coarse  $\sqrt{f}$  EQL. The  $\sqrt{f}$  EQL gain is automatically controlled so that the post-filter output level approaches the reference level.

### III. COARSE $\sqrt{f}$ EQL TRANSFER FUNCTION APPROXIMATION

#### A. Sampling Frequency

In order to realize high-frequency SC equalizer circuits with a low power consumption, as well as a small chip area, a total amount of capacitances must be well reduced. On the other hand, the capacitor ratio range is proportional to both a sampling frequency and equalizer gain. Therefore, it is desirable to reduce a sampling frequency and to divide a total gain into the equalizer and other blocks. In such a case, however, circuit complexity for both analog pre- and post-filters may be increased. Specifications for these filters are determined from anti-aliasing the 50-percent duty pulse spectrum and channel noises, and smoothing the SC filter output waveform so as to precisely detect the top or bottom and zero cross points. An useful approach to simplify these analog filters is to employ a low-order SC low-pass filter with a higher clock rate than that for the equalizer [10]. For example, the pre-filter can be constructed as a combined form of a second-order active RC filter and a second-order SC filter. The post-filter is also simplified by operating the roll-off filter with a high sampling frequency.

For these reasons, the sampling frequency for the equalizer is chosen to be relatively low, that is four times as high as data bit rate.

#### B. Pole-Zero Location

An example of the transmission line characteristics is shown in Fig. 2. Next, pole-zero locations, which are adopted for equalizing these amplitude and group delay responses, are illustrated in Fig. 3. A major part of the equalizer response is formed with  $Z_1$ . The characteristics in the low- and middle-frequency bands are further compensated for by using  $Z_2$  and  $P_1$ . The reason  $Z_2$  is located

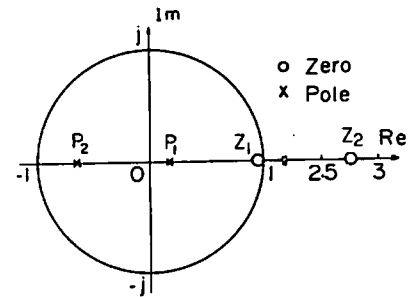


Fig. 3. Pole-zero locations for coarse  $\sqrt{f}$  EQL transfer function.

outside the unit circle is explained as, the transmission group delay distortions being somewhat smaller than group delay distortions in the minimum phase system. Pole  $P_2$  located on the negative real axis is used to form amplitude response in the high-frequency band.

The pole-zero location illustrated in Fig. 3 is used to equalize the line characteristics shown in Fig. 2. The location of this pole-zero location for arbitrary line length is determined through the actual design process. For different types of lines and frequency bands, optimum pole-zero locations must be further discussed based on the relationship between line amplitude and group delay response.

#### C. Approximation Algorithm

Data transmission quality is directly evaluated by the error rate in terms of a signal-to-noise ratio. It is equivalently estimated by intersymbol interference in an isolated pulse response. The proposed algorithm, therefore, approximates a transfer function by using poles and zeros, given in Fig. 3, as variables and ISI as an error criterion.

Let  $g(t)$  be an isolated pulse response for the whole system shown in Fig. 1, which does not, however, include the coarse  $\sqrt{f}$  EQL. The other filters are determined in advance, and are fixed in the time domain approximation. Furthermore, an impulse response for the coarse EQL is denoted by  $h(t)$ . Then an isolated pulse response for the whole system can be expressed as

$$f(t) = \int_0^t h(\tau) g(t - \tau) d\tau. \quad (1)$$

Letting  $T_0$  be a sampling point at which  $f(t)$  has its maximum value, the received pulses are sampled at  $t_n$  given by

$$t_n = T_0 + nT, \quad n = \text{integer} (\neq 0) \quad (2a)$$

$$T = 1/f_0, \quad f_0: \text{data rate}. \quad (2b)$$

ISI is usually evaluated by an absolute sum of the root mean square of  $f(t_n)$ . The absolute sum estimates the worst case, and closely relates to the mean square error. Hence, it is employed as an error criterion expressed by

$$E = \sum_{\substack{n=-n_1 \\ n \neq 0}}^{n_2} w(n) |f(t_n)/f(T_0)| \quad (3)$$

where  $w(n)$  is a weighting coefficient.

The proposed algorithm minimizes  $E$  through an iterative method, which locally employs a linear programming technique. In the following discussions, the poles and zeros are denoted by

$$\begin{aligned} x_1 &= Z_1 \\ x_2 &= Z_2 \\ x_3 &= P_1 \\ x_4 &= P_2. \end{aligned} \quad (4)$$

Let a vector consisting of  $x_i$  be  $x$ , and  $x$  at the  $r$ th iteration step be expressed as  $x^{(r)}$ . The isolated pulse response  $f(t)$  using  $x^{(r)}$  is denoted by  $f(x^{(r)}, t)$ . When deviations in  $x^{(r)}$  are assumed to be sufficiently small,  $\Delta x^{(r)} \ll 1$ ,  $f(x^{(r)} + \Delta x^{(r)}, t_n)$  is approximately expressed as

$$f(x^{(r)} + \Delta x^{(r)}, t_n) \approx f(x^{(r)}, t_n) + \sum_{i=1}^K \Delta x_i^{(r)} \left( \frac{\partial f(x, t_n)}{\partial x_i} \right)_{x=x^{(r)}}. \quad (5)$$

If  $x^{(r)}$  is assumed to be constant,  $f(x^{(r)}, t_n)$  and  $(\partial f(x, t_n)/\partial x_i)_{x=x^{(r)}}$  also become constant and, consequently, (5) can be regarded as a linear combination of  $\Delta x_i^{(r)}$ . Equation (5) is rewritten as

$$f(x^{(r)} + \Delta x^{(r)}, t_n) = A_n^{(r)} + \sum_{i=1}^K B_{n,i}^{(r)} \Delta x_i^{(r)} \quad (6)$$

where

$$A_n^{(r)} = f(x^{(r)}, t_n) \quad (7a)$$

$$B_{n,i}^{(r)} = \left( \frac{\partial f(x, t_n)}{\partial x_i} \right)_{x=x^{(r)}}. \quad (7b)$$

Next, the absolute sum of  $f(x^{(r)}, t_n)$ , given by (3), is expressed as a linear combination of  $f(x^{(r)}, t_n)$  by using sign coefficients  $\delta(n)$  expressing the polarity of  $f(x^{(r)}, t_n)$  as follows:

$$E^{(r)} = \sum_{\substack{n=n_1 \\ \neq 0}}^{n_2} \delta(n) w(n) f(x^{(r)}, t_n) \quad (8a)$$

$$\delta(n) = \begin{cases} 1, & 0 \leq f(x^{(r)}, t_n) \\ -1, & f(x^{(r)}, t_n) < 0 \end{cases} \quad (8b)$$

where  $|f(x^{(r)}, T_0)|$  is normalized as unity. From (6) and (8), minimizing  $E$  can be formulated as follows:

$$0 \leq \delta(n) \left( A_n^{(r)} + \sum_{i=1}^K B_{n,i}^{(r)} \Delta x_i^{(r)} \right) \quad (9a)$$

$$\tilde{E}^{(r)} = \sum_{\substack{n=n_1 \\ \neq 0}}^{n_2} \delta(n) w(n) \left( A_n^{(r)} + \sum_{i=1}^K B_{n,i}^{(r)} \Delta x_i^{(r)} \right) \quad (9b)$$

$$\tilde{E}^{(r)} \rightarrow \text{Minimized.} \quad (9c)$$

Since (9) is expressed as a linear equation in  $\Delta x_i^{(r)}$ , this problem can be reduced to the linear programming. In (9),

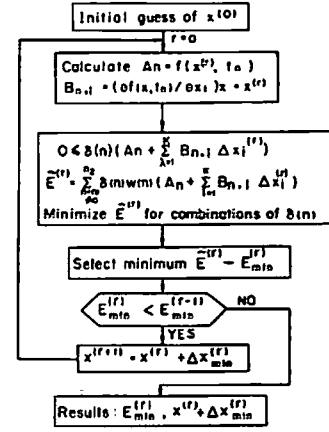


Fig. 4. Approximation algorithm for coarse  $\sqrt{f}$  EQL transfer

solved for all possible combinations of  $\delta(n)$ . In applications, however, useful combinations can be to some extent.

Among the solutions, the minimum  $\tilde{E}^{(r)}$  and the responding variable  $\Delta x^{(r)}$  are chosen. They are denoted  $E_{\min}^{(r)}$  and  $\Delta x_{\min}^{(r)}$ , respectively. The initial values,  $(r+1)$ th iteration step, are given by

$$x^{(r+1)} = x^{(r)} + \Delta x_{\min}^{(r)}.$$

At the  $(r+1)$ th step, the same procedure is repeated the iteration step, where  $E_{\min}^{(r+1)} < E_{\min}^{(r)}$  is not held. When the approximation is completed, a general flow chart of the proposed algorithm is given in Fig. 4.

#### Frequency Response

After the time domain approximation, the gain Nyquist frequency ( $f_N = f_0/2$ ) is adjusted to the specified level. Actual gain levels for the coarse  $\sqrt{f}$  EQL are set down in order to compress the capacitor ratio range. The shifted gain level is compensated for by other blocks.

#### Monotonic Capacitor Values

When variable capacitor values monotonically increase or decrease in ascending order of the equalizer gain control circuit becomes very simple. For this purpose, poles and zeros are constrained so as to monotonically increase or decrease, according to the equalizer gain in the approximation process.

## IV. DESIGN OF FINE EQUALIZER

### A. Gain Adjust

Fig. 5 shows two approaches *A* and *B* to combine responses of the coarse  $\sqrt{f}$  EQL and fine EQL. Let  $i$  and  $j$ , respectively, a combined step is denoted by  $k$ . Furthermore, the zeroth and  $(N-1)$ th steps correspond to the minimum and maximum gain levels, respectively. Amplitude responses at the  $(m-1, N-1)$ th and  $(0, 0)$ th steps become short and over equalizations, in the  $\sqrt{f}$  characteristic, respectively. Effects of these deviations on the isolated pulse response were investigated by computer simulation. The results show the short and

I. Goin

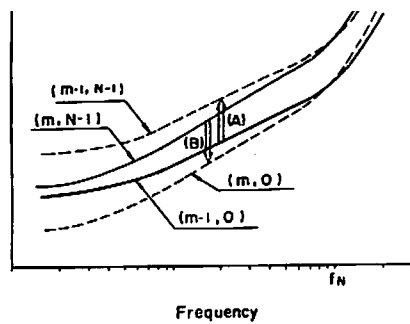


Fig. 5. Two approaches to combining coarse  $\sqrt{f}$  EQL and fine EQL step responses.

ing many data sampling points. On the other hand, negative deviation, caused by the over equalization, is mainly concentrated within two time slots. This deviation is effectively cancelled by a decision feedback equalizer with a few taps [7]. Therefore, the approach B is employed.

In the coarse  $\sqrt{f}$  EQL transfer function approximation, the fine EQL is fixed to the  $(N-1)$ th step.

### B. Delay Time Adjust

Another problem of the step variable equalizer is delay time difference. The delay time differences between the adjoining step responses of the coarse  $\sqrt{f}$  EQL result in timing jitter and degrade error rate quality. The fine EQL purposes include compensation for this difference. The adjoining combination steps, where the coarse  $\sqrt{f}$  EQL step response is changed, are expressed as  $(m-1, N-1) \rightleftharpoons (m, 0)$ . Letting  $\Delta T_{m-1, m}$  be the delay time difference between the  $(m-1)$ th and  $m$ th coarse  $\sqrt{f}$  EQL steps, it can be completely compensated for by designing the fine EQL so that the delay time difference  $\Delta t_{N-1, 0}$  between the  $(N-1)$ th and 0th steps satisfies

$$\Delta T_{m-1, m} + \Delta t_{N-1, 0} = 0. \quad (11)$$

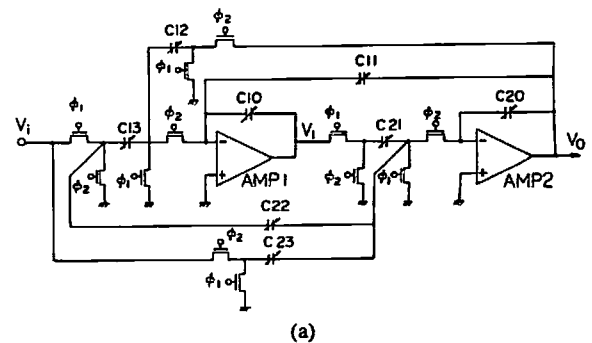
In actuality, however,  $\Delta T_{m-1, m}$  slightly differs from step to step. Therefore, the mean value for  $\Delta T_{m-1, m}$ ,  $1 \leq m \leq N-1$ , is reduced to zero. Furthermore, delay times for the intermediate steps of the fine EQL are determined so as to gradually vary.

The fine EQL is designed using a first-order transfer function having only one pole.

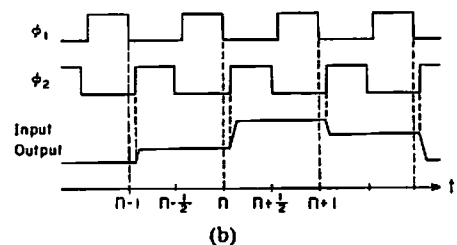
## V. CIRCUIT CONFIGURATIONS

### A. Coarse $\sqrt{f}$ Equalizer

The transfer function with the poles and zeros given in Fig. 3 can be synthesized by using the  $E$  circuit among a family of active SC biquads [12]. The circuit configuration and its transfer functions are given in Fig. 6 and by (12), respectively.



(a)



(b)

Fig. 6. (a) Circuit configuration for coarse  $\sqrt{f}$  EQL. (b) Clock and sampling points.

$$\frac{V_0}{V_i} = - \frac{C_{23} - (C_{23} + C_{22})z^{-1} + (C_{22} - C_{21}C_{13})z^{-2}}{1 + (C_{21}C_{12} + C_{21}C_{11} - 2)z^{-1} + (1 - C_{21}C_{11})z^{-2}}$$

$$C_{10} = C_{20} = 1.$$

Variable capacitors are constructed as a programmable capacitor array, as shown in Fig. 7. Appropriate capacitors are selected through switches to realize a variable capacitor in a parallel form. Since the variable capacitor values are designed so as to vary in ascending or descending orders, according to increasing the gain level, the differences between the adjoining capacitors are prepared as the branch capacitors. The control signals also become very simple in this way.

This kind of variable SC equalizer usually causes undesirable responses, such as spike and transient response, at the instant of discretely changing the capacitor values. The object of the present study, however, is limited to the compression multiplexed bidirectional transmission mentioned previously. Therefore, the above response can be prevented by changing the capacitors during a timing mode in which the  $\sqrt{f}$  EQL is not used.

### B. Fine Equalizer

Fig. 8 shows the circuit configuration for the fine equalizer with one pole. The transfer function is expressed by

$$\frac{V_0}{V_i} = \frac{C_{12}z^{-1}}{C_{11} + C_{10}(1 - z^{-1})}. \quad (12)$$

Gains at the Nyquist frequency and delay time are controlled by  $C_{12}$  and  $C_{10}$ , respectively.

$$\frac{V_1}{V_i} = - \frac{(C_{23}C_{12} + C_{23}C_{11}) + (C_{13} - C_{22}C_{12} - C_{22}C_{11} - C_{23}C_{11})z^{-1} + (C_{11}C_{22} - C_{13})z^{-2}}{1 + (C_{21}C_{12} + C_{21}C_{11} - 2)z^{-1} + (1 - C_{21}C_{11})z^{-2}} \quad (13)$$

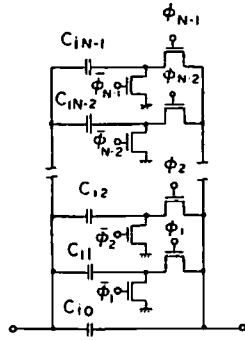


Fig. 7. Variable capacitor array.

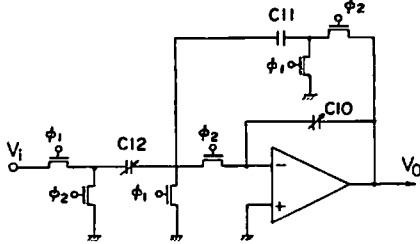


Fig. 8. Circuit configuration for fine EQL.

## VI. DISCRETE OPTIMIZATION OF CAPACITOR VALUES

### A. Integer Value Capacitors

In order to achieve high accuracy capacitor ratios using small capacitors on monolithic MOS circuits, it is desirable to realize arbitrary capacitors with a plural number of the same dimensional unit capacitors. In this case, capacitor values are equivalently represented to integer values. The integer value capacitors also make it possible to simplify the programmable capacitor array and the control signals.

### B. Discrete Optimization Algorithm

Positive real capacitors, obtained from (12) and through scaling the operational amplifier outputs, are rounded off into discrete values. The roundoff error effects on the SC equalizer response have to be minimized [13].

Since discretely searching for optimum capacitors usually requires a large number of computations, the pole and zero deviations are employed as an error criterion instead of ISI.

Let the poles and zeros obtained through the time domain approximation in Section III and rounding off capacitor values be  $x_i$  and  $x_{Ri}$ , respectively. The distance between  $x_i$  and  $x_{Ri}$ , which is defined by

$$D = \sum_{i=1}^K w_i |x_i - x_{Ri}| \quad (14a)$$

$$w_i = \frac{1}{|1 - x_i|}, \quad 0 \leq x_i \quad (14b)$$

$$= \frac{1}{|1 + x_i|}, \quad x_i < 0 \quad (14c)$$

is employed as an error criterion. A weighting coefficient  $w_i$

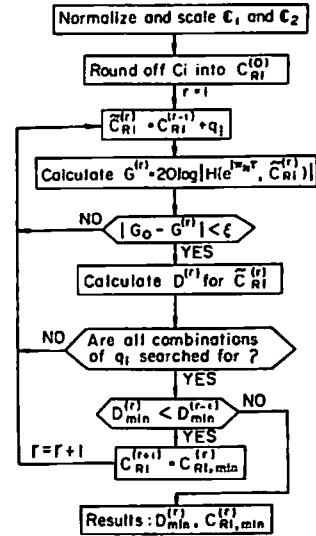


Fig. 9. Discrete value capacitor optimization algorithm.

The capacitors in the SC biquad shown in Fig. 6 divided into two groups,

$$C_1 = (C_{10}, C_{11}, C_{12}, C_{13}) \quad (15)$$

$$C_2 = (C_{20}, C_{21}, C_{22}, C_{23}). \quad (16)$$

Since the SC circuit performances valid for  $C_1$  and multiplied by constants, they are first scaled by propriate constants  $R_1$  and  $R_2$ , and are rounded off integer values. These scaling factors are determined by lower bound for integrator capacitors and the round error effects, and the upper bound for a total amount of capacitances.

Let the initially rounded off capacitor values be  $C_{Ri}^{(0)}$ . At the 1st step, the optimum capacitances are discretely searched for around  $C_{Ri}^{(0)}$ .

Letting

$$\tilde{C}_{Ri}^{(1)} = C_{Ri}^{(0)} + q_i$$

where,  $q_i$  is an integer in the restricted region, the criterion  $D$  given by (14) is calculated for all possible combinations of  $\tilde{C}_{Ri}^{(1)}$ . Among the above  $D^{(1)}$ , the minimum  $D^{(1)}$  and the corresponding  $\tilde{C}_{Ri}^{(1)}$  are selected. They are denoted as  $D_{min}^{(1)}$  and  $C_{Ri, min}^{(1)}$ , respectively.  $C_{Ri, min}^{(1)}$  is used as the initial capacitance at the 2nd step, as expressed by (16) and the same searching procedure is repeated.

$$\tilde{C}_{Ri}^{(2)} = \tilde{C}_{Ri, min}^{(1)} + q_i.$$

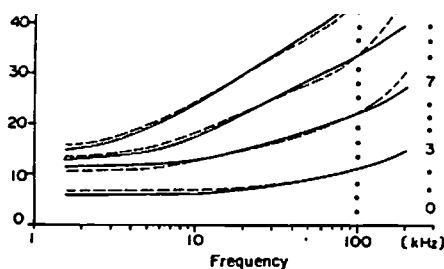
At the step where  $D_{min}^{(r+1)} < D_{min}^{(r)}$  is not held, the discrete optimization is completed.

Tolerance is imposed on the equalizer gain at the Nyquist frequency. The capacitor combinations, with which gains meet the given tolerance, are only adopted for final evaluation of  $D$ .

The algorithm described above is shown as a flowchart in Fig. 9.

## VII. DESIGN EXAMPLES

The line equalizer system was designed for 200

Fig. 10. Amplitude responses in decibels for coarse  $\sqrt{f}$  EQL.

loss at 100 kHz. Sixteen kinds of step responses are assigned to both the coarse  $\sqrt{f}$  EQL and the fine EQL. Hence, 256 step responses can be realized as a whole, and gain difference becomes about 0.2 dB ( $\approx 45$  dB/256 steps).

#### A. Coarse $\sqrt{f}$ EQL

##### Transfer Function Approximation:

In the time-domain approximation, ISI is evaluated in the interval from  $T_0 - 2T$  to  $T_0 + 5T$ , that is  $n_1 = -2$  and  $n_2 = +5$ , and  $w(n)$  values are chosen to be unity for all sampling points. The resulting ISI is less than 9 percent for all step responses. Examples of amplitude responses in decibels are shown in Fig. 10.

##### Discrete Optimization:

The capacitor values were discretely optimized using the scaling factors,  $R_1 = 4$  and  $R_2 = 8^1$  in the region of  $C_{R_i}^{(r)} + q_i$ ,  $-3 \leq q_i \leq +3$ , which has seven grids for each capacitor. The tolerance for the gain deviation at 100 kHz is 0.3 dB. In the 15th step response, for instance, a gain of 15.07 dB (target: 14.90 dB, which is shifted down by 30.1 dB) and pole-zero deviation of 9.1 percent after only rounding off are improved to 14.94 dB and 2.7 percent, respectively. Degradations on the eye openings after optimization are very small.

##### Capacitor Ratio Range:

The coarse  $\sqrt{f}$  EQL gain levels for three groups of step responses, that is 0–5th, 6–10th, and 11–15th steps, are shifted by  $-6.0$ ,  $-18.1$ , and  $-30.1$  dB, respectively. As a result of the 800 kHz sampling frequency and the above gain level shift, the capacitor ratio ranges<sup>2</sup> for  $C_1$  and  $C_2$  are reduced to 27.8 and 12.6, respectively, over all steps.

#### B. Fine EQL

Three kinds of group delay responses were designed for the fine EQL. At the same time, the gain at 100 kHz is equally divided by about 0.2 dB steps. The amplitude responses are shown in Fig. 11. Delay time differences between the adjoining coarse  $\sqrt{f}$  EQL step responses are

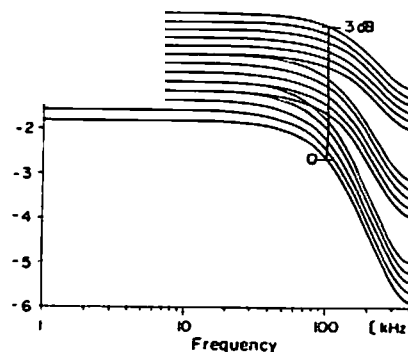


Fig. 11. Amplitude responses in decibels for fine EQL.

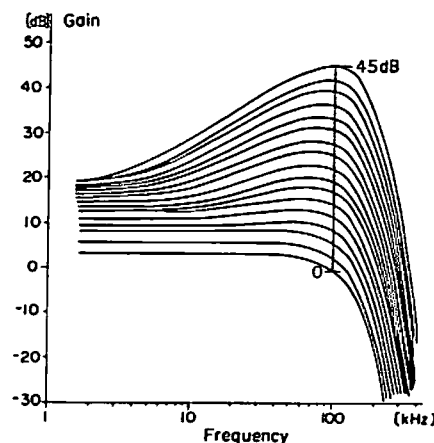


Fig. 12. Amplitude responses in decibels for line equalizer.

up to  $0.34 \mu\text{s}$ , which is 6.8 percent of a data period  $5 \mu\text{s}$  ( $=1/200$  kHz), and is not negligible. Delay time difference is compressed to  $0.14 \mu\text{s}$  (0.28 percent of a data period).

#### C. Line Equalizer System

The pre-filter is synthesized by combining a second-order RC active filter and a second-order SCF with a sampling frequency than 800 kHz. The cutoff ( $-3$  dB) was determined to be 300 kHz, taking errors into account. The post-filter is a third-order RC active filter having a 270-kHz cutoff frequency. The filter is realized with a fourth-order SCF having approximate 100-percent roll-off cosine amplitude response. Amplitude responses for the line equalizer system including the filters and the  $\sqrt{f}$  EQL, are given in Fig. 12. Furthermore, frequency responses for a whole system including a 50-percent duty rectangular pulse transmission line with the maximum length, are given in Fig. 13. This figure shows that an approximate 100-percent cosine roll-off response is obtained for a whole system. Fig. 14 shows a calculated eye opening corresponding to the frequency responses in Fig. 13. When an eye opening is measured by a ratio of the inside and outside eye widths for the eye opening, the rates for all step responses are greater than 80 percent.

Suzuki *et al.* [6] reported a simplified equalizer effectively combining a second-order  $\sqrt{f}$  EQL and

<sup>1</sup>Capacitor values before scaling, are normalized so that the minimum value is unity.

<sup>2</sup>The capacitor ratio range means a ratio of the maximum and minimum capacitances in this paper.

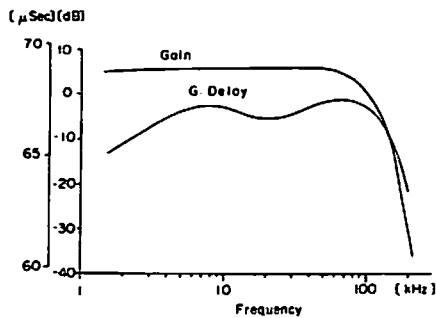


Fig. 13. Amplitude and group delay responses for a whole system including pulse waveform, 0.5-mm $\varnothing$  line with 5.9-km length and line equalizer system having the maximum gain level 45 dB at 100 kHz.

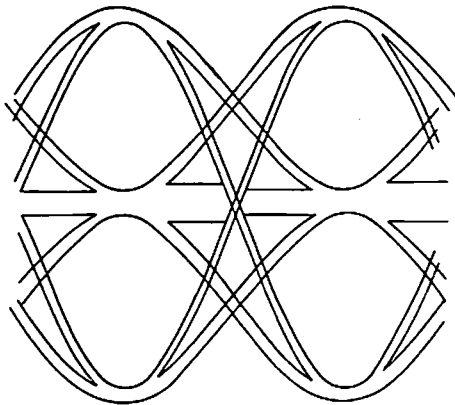


Fig. 14. Calculated eye pattern corresponding to the frequency responses shown in Fig. 13.

order roll-off filter. Since data is detected at the SC equalizer output, the clock phase should be synchronized to the bit rate (200 kHz) so that the top or bottom of the waveform is just sampled [14]. On the other hand, in our approach, the SC circuits operate with asynchronous clock phase, and the sampled and held waveform must be well smoothed before data detection. In addition to this, a high gain SC equalizer system is expected to induce relatively large various kinds of noises. For these reasons, higher stopband attenuation is assigned to the roll-off filter compared with the above approach [6]. Furthermore, in order to simplify programmable capacitor arrays and control circuits, the roll-off filter response is fixed.

#### D. LSI Implementation

The designed line equalizer system was fabricated using 3- $\mu$ m CMOS technology [15]. The measured data are very close to the designed performances. An example of the measured eye opening for a 5.9-km long 0.5-mm $\varnothing$  transmission line is shown in Fig. 15.

### IX. CONCLUSION

Design techniques for a SC adaptive line equalizer have been proposed. Particularly, this paper has placed stress on the following subjects. They include optimum pole-zero location, transfer function approximation in a time do-

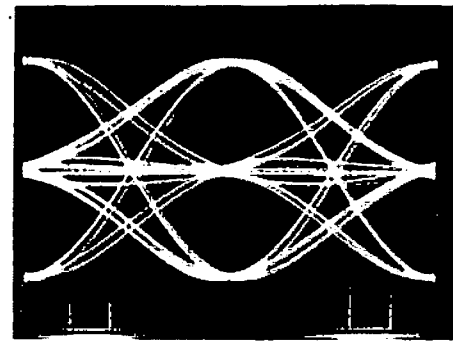


Fig. 15. Measured eye pattern for 0.5-mm $\varnothing$  line with 5.9 km

time differences. The line equalizer system, which applied to 200 kb/s digital transmission over the 0.5-line, was designed through the proposed method. Desirable performances were obtained. An LSI was fabricated using 3- $\mu$ m CMOS technology. The measurements were very close to the calculated performances.

### ACKNOWLEDGMENT

The authors wish to thank M. Hibino, M. Nakajima, Sakamura, and M. Yamaguchi of NEC Corporation for their valuable suggestions and continuous encouragement.

### REFERENCES

- [1] S. V. Ahamed, P. P. Bohn and N. L. Gottfried, "A two-wire digital transmission in the loop plant," *IEEE Commun.*, vol. COM-29, pp. 1554-1564, Nov. 1981.
- [2] N. Inoue, R. Komiya, and Y. Inoue, "Time-shared two-wire subscriber transmission system and its application to the telephone set," *IEEE Trans. Commun.*, vol. COM-29, pp. 1565-1572, Nov. 1981.
- [3] H. Ogiwara and Y. Terada, "Design philosophy and implementation for digital subscriber loops," *IEEE Trans. Commun.*, vol. COM-30, pp. 2057-2065, Sept. 1982.
- [4] R. W. Brodersen, P. R. Gray, and D. A. Hodges, "MOS switched capacitor filters," *Proc. IEEE*, vol. 67, pp. 61-75, Jan. 1979.
- [5] K. Martin and A. S. Sedra, "Switched-capacitor building blocks for adaptive systems," *IEEE Trans. Circuits Syst.*, vol. CAS-28, pp. 576-584, June 1981.
- [6] T. Suzuki *et al.*, "A CMOS switched-capacitor variable equalizer," *IEEE Trans. J. Solid-State Circuits*, vol. SC-18, pp. 700-706, Dec. 1983.
- [7] M. Ishikawa, T. Kimura and N. Tamaki, "A CMOS adaptive equalizer," *IEEE J. Solid-State Circuits*, vol. SC-19, pp. 707-714, Oct. 1984.
- [8] D. J. Allstot, R. W. Brodersen, and P. R. Gray, "An electrically programmable switched capacitor filter," *IEEE J. Solid-State Circuits*, vol. SC-14, pp. 1034-1041, Dec. 1979.
- [9] K. Nakayama, Y. Takeuchi, and Y. Kuraishi, "Design of a switched capacitor adaptive line equalizer (in Japanese)," *IECE Japan Tech. Meeting on Circuits and Sys.*, CAS 84-10, pp. 9-11, 1984.
- [10] K. Nakayama, Y. Ishikawa, and Y. Kuraishi, "Design of a speech spectrum analyzer using switched capacitor filter technique," *Proc. ICASSP'83*, pp. 515-518, 1983.
- [11] K. Nakayama, Y. Sato, and Y. Okuyama, "On pole-zero location of SC line equalizer (in Japanese)," *IECE Japan, National Conference*, p. 2085, Mar. 1985.
- [12] P. E. Fleisher and K. R. Laker, "A family of active switched capacitor biquad building blocks," *Bell Syst. Tech. J.*, vol. 58, pp. 2235-2269, Dec. 1979.
- [13] S. Fushimi and K. Nakayama, "A discrete optimization method for switched capacitor filters (in Japanese)," *IECE Japan, Trans. J.*, pp. 580-587, June 1984.
- [14] T. Suzuki, H. Takatori, and F. Fujii, "A CMOS line equalizer for digital subscriber loop," in *ISSCC Dig. Tech. Papers*, pp. 2-3, Feb. 1984.
- [15] K. Nakayama, Y. Takeuchi, Y. Kuraishi, and T. Sato, "A CMOS adaptive line equalizer," in *ISSCC Dig. Tech. Papers*, pp. 2-3, Feb. 1984.



Simulation of NEQ Generation in 1983,  
ent  
ps.  
ro-

on  
in

Yayoi  
Univ

and